We are IntechOpen, the world's leading publisher of Open Access books Built by scientists, for scientists

6,900
Open access books available

186,000
International authors and editors

200M
Downloads

Our authors are among the

154
Countries delivered to

TOP 1%
most cited scientists

12.2%
Contributors from top 500 universities

CLARIVATE ANALYTICS
BOOK CITATION INDEX
INDEXED

WEB OF SCIENCE™

Selection of our books indexed in the Book Citation Index
in Web of Science™ Core Collection (BKCI)

Interested in publishing with us?
Contact book.department@intechopen.com

Numbers displayed above are based on latest data collected.
For more information visit www.intechopen.com

Fabrication and Characterization of Metal-Loaded Mixed Metal Oxides Gas Sensors for the Detection of Hazardous Gases

Chang-Seop Lee and Yong Jae Kim

Additional information is available at the end of the chapter

Abstract

This study concerns gas sensors that may protect individuals by detecting hazardous gases that may be generated in hot spaces (≥50°C) with residues of organic waste. We investigated the responses and selectivities of the sensors to different kinds of hazardous gases such as acetaldehyde, toluene and hydrogen sulfide. We also investigated operating temperatures and catalysts for the sensors. The thick film semiconductor sensors that detected some hazardous gases were prepared using nano-sized sensing material powders (SnO_2, WO_3, ZnO) that were prepared through sol-gel and precipitation methods. The nano-sized sensing materials were blended with various amounts of metal oxides (SnO_2, ZnO, WO_3) and coated with transition metals (Pt, Pd, Ru, Au, Ag, Cu and In). The metal oxide thick films were fabricated on an Al_2O_3 plate with a Ni-Cr heater and a Pt electrode through a screen-printing method. Morphologies, compositions, phases, surface areas and particle sizes of sensor compounds were examined by SEM, EDS, XRD and BET analysis. The investigated response to the various hazardous vapors was expressed as the value of Ra/Rg, where Ra and Rg are the resistance of the sensor material in the air and in hazardous gas, respectively.

Keywords: gas sensors, hazardous gas, metal oxide, screen-printing, sol-gel, thick film

1. Introduction

The semiconducting metal oxide gas sensors currently constitute one of the most investigated groups of gas sensors. Semiconducting metal oxide gas sensors are electrical conductivity sensors with active sensing layers that exhibit resistance changes when coming into contact with the hazardous gas under investigation. Metal oxide gas sensors are appropriate for a

wide range of applications and for the detection of all reactive gases due to unique atomic-level chemistry and properties of each device.

Hydrocarbons, nitrogen oxides, oxidized hydrocarbons and sulfur oxides are common air contaminants in everyday life. Of these chemicals, hazardous gases produced from organic solvents used in industrial and laboratory processes are becoming an area of increasing social concern, since those vapors have a direct damage on the human body. Acute and chronic exposures to hazardous gases may cause humans to develop central nervous system disorders, reproductive system diseases and leukemia [1–3].

Formaldehyde and acetaldehyde are known to be two of the carbonyl compounds most widely disseminated in ambient air. Aldehydes products produced by combustion and oxidation can interact directly with ozone. The products are major components of smog, and further photochemical reactions may enhance global warming by destroying ozone layer in the stratosphere. Aldehydes commonly present in the gaseous state at 25°C and stay in the air for a long period of time. Acetaldehyde is the main component of hazardous vapor produced in newly built houses and can pollute the air both outdoors and indoors. Humans exposed to aldehydes irritations to their respiratory systems such as their throats, noses and bronchi. In addition, acetaldehyde may affect the central nervous system of an individual via anesthesia. Extreme physical reactions such as paralysis, respiratory disorders, and even the onset of a comatose state are among the events that can occur in extreme cases of acetaldehyde exposure [4, 5]. Therefore, for both environmental and for health reasons, it is very important to detect the presence of aldehydes.

Hydrogen sulfide, a byproduct of the active decomposition of organic matter, is very hazardous gas. For instance, many people died in the underground sewage systems of Paris during the French Revolution. According to the U.S. government report, H_2S is a watchful gas for instant death in the working place. Because H_2S gas is rapidly oxidized into sulfides that can easily be eliminated via the kidneys, the gas is not known to have a cumulative toxic effect. Inhalation of lethal concentrations (1000–2000 ppm) of hydrogen sulfide may cause olfactory fatigue or paralysis and ultimately the cessation of breath. Other forms of respiratory distress known to occur after inhalation of hydrogen sulfide (500–1000 ppm) are dose-dependent deficits such as hyperpnea (via carotid body stimulation) and sleep apnea. Low levels of hydrogen sulfide (50–500 ppm) can act as primary irritants to the eyes and the respiratory system. Continuous exposure to 250–600 ppm of the hazardous gas may result in pulmonary edema.

Toluene is a colorless volatile liquid with a unique smell. Safe handling of this highly volatile compound includes storage in a perfectly sealed container. If toluene is handled in an industrial workplace or in a laboratory without wearing special protective equipment, a worker or researcher may inhale 100% of the toluene. Prolonged inhalation exposure to toluene, even at low concentrations, can lead to deterioration of lung function and eyesight. Additional effects include a headache, paralysis of the hands/feet, cancer, leukemia, mental derangement, malignant lymphoma and depression of central nervous system.

In this chapter, we describe the development of catalyst-loaded metal oxide gas sensors to detect gases that posed hazards to the human body, that is, acetaldehyde gas, hydrogen sulfide and toluene vapors.

2. Experimental details

2.1. Preparation of sensor materials

One of the disadvantages of gas sensors is the costly requirement for more electricity to maintain a high operating temperature. To mitigate this disadvantage, there is a need to increase the electronic conductivity of the sensor materials in order to decrease the operating temperature. One way to improve the electronic conductivity is to add conducting materials to sensor materials.

For the acetaldehyde gas sensor, we synthesized WO_3 through a sol-gel process and used it as a sensing material to detect acetaldehyde gas. Metal catalysts were added through the impregnation method [4–6], to enhance the sensitivity and selectivity that are functional prerequisites of the gas sensor. Transition metals (Pd, Ru, Pt and In) were weighed to give weight ratios of 1–5 wt%, and 1 ml of hydrochloric acid (HCl) diluted with distilled water was added to completely dissolve the metal catalysts in a beaker. Heating and stirring of appropriate suspensions with magnetic stirrers yielded WO_3 or SnO_2/WO_3 powders impregnated with metal catalysts. Then, we dried each solution for 12 h at 100°C and calcined it for 2 h at 500°C to get powder. Finally, we obtained a fine powder of the sensing material by crushing the crude material.

We added metal catalysts to WO_3/SnO_2 powder to prepare the sensing material by using the same methods described above in the case of the hydrogen sulfide sensor. Additional techniques included co-precipitation, impregnation method and alleged fabrication [6]. We put various metals of Pd, Ru, Ag, Au and In as catalysts in the flask with the ratios of 0.5–5 wt% and dissolved the metal catalysts by adding 1 ml of concentrated HCl solution. We then added SnO_2/WO_3 powder to impregnate the metal catalysts. These materials were slowly heated while stirring with a magnetic stirrer for an effective loading of metal catalysts to SnO_2/WO_3. The as-prepared sample was then dried for 24 h at 110°C and calcinated for 2 h at 600°C. Finally, the sample was pulverized to make each one of the sensor materials.

In the case of the toluene sensor, we produced a sensor material by adding carbon black using an impregnation method. An impregnation method was also used for the addition of the transition metal. Carbon black was measured to be at 1–20 wt.% of the main material. Then, it was put into a beaker and 2 ml of HCl was added. After transition metal and carbon black are completely dissolved, distilled water was added to make a homogeneous solution. Next, the transition metal and carbon black were impregnated by adding SnO_2/ZnO powder. Then, it was gradually heated while stirring with a magnetic stirrer to produce $SnO_2/ZnO/catalyst$ powder with carbon black deposit. The powder was dried for 24 h at 110°C and went through calcination for 5 h at 600°C. The desired material was obtained by crushing the obtained powder [7–11].

2.2. Fabrication of thick film

A commercial product which has Pt electrode at 0.5-mm interval and a Ni-Cr heater in a 10 mm × 8 mm × 0.65 mm Al_2O_3 base plate was used as the supporting material for the sensor. The plate went through a washing process using an acetone and heat treatment process at 300°C for 1 h in order to remove contaminants before fabrication of the thick film. Next,
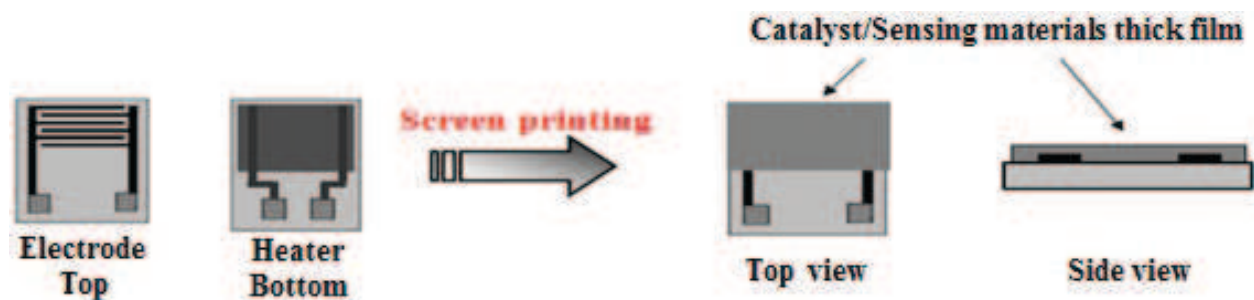
Figure 1. Structure of thick film sensor.

the sensor material paste was coated by a screen-printing method at a thickness of 20–60 μm. **Figure 1** shows diagrams before and after coating of the thick films [12].

Regarding thick film formation on each sensor material, a paste with proper viscosity was screen-printed on an alumina base plate with electrode formation achieved by adding ethylene glycol as a binder at 15–30 wt.% of powder. The resulting thick film element was left at room temperature for 12 h. Then, it was dried for 24 h in an 110°C oven. After 2 h calcination at 600°C, the final product was obtained.

2.3. Analysis of sensitivity characteristics

After we had installed the gas sensor at a distance of 50 mm from the bottom of a 10 L (250 mm x 200 mm x 200 mm) chamber, the sensitivity of the gas sensor was measured with the temperature range from 200 to 400°C. A stabilization procedure was performed for 12 h in the
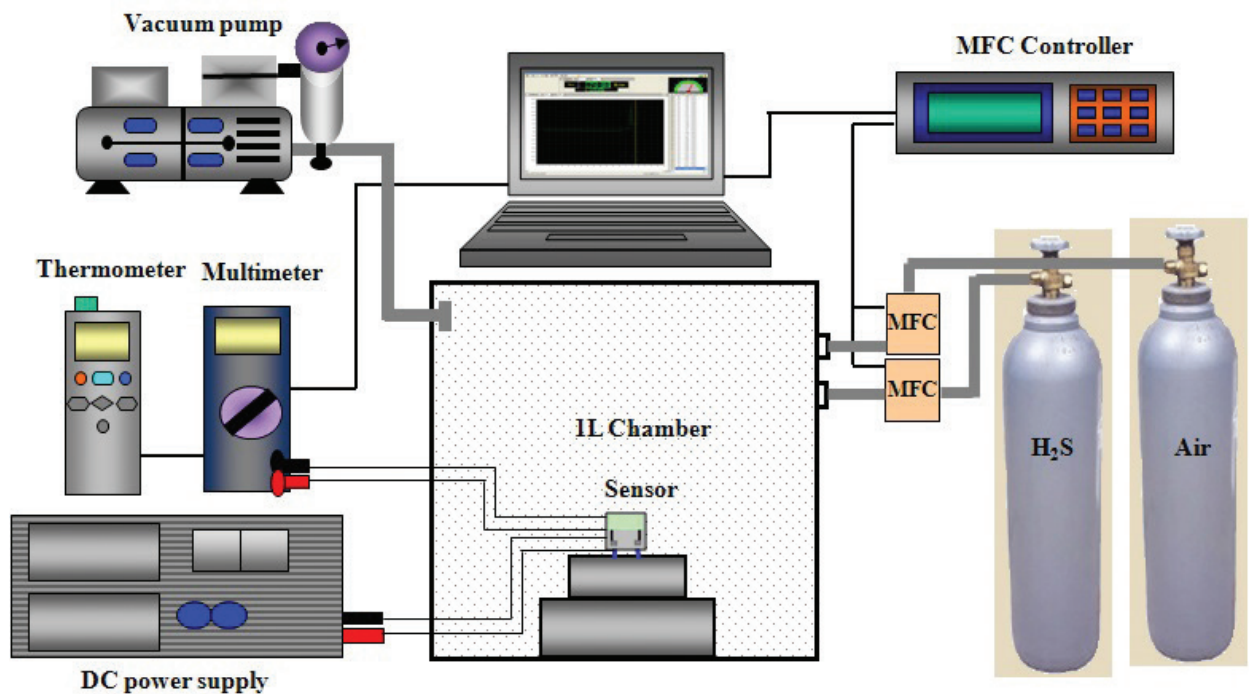

Figure 2. Apparatus used for gas-sensing experiments.

same temperature range to remove the electrons from the system. Then, the target gas had been dispersed using a fan in the chamber. When the equilibrium concentration was reached, the resistance was measured with an electrometer. The sensor sensitivity was expressed as the value of Ra/Rg, where Ra and Rg are the resistance of the sensor material in the air and in target gas, respectively. The experimental apparatus is shown in **Figure 2**.

3. Results and discussion

3.1. Analysis results of sensing materials used for the gas sensor

3.1.1. The acetaldehyde gas sensor

In this study, we prepared sensing materials for a gas-detecting sensor using various composition ratios of WO_3 powder employed as the main sensing element to metal oxide (SnO_2) and metal catalysts. XRD, SEM/EDS and BET methods were employed to characterize the crystallinity and morphology, phase, composition and specific surface areas. The XRD patterns of WO_3 at various calcination temperatures and those when SnO_2 and metal catalysts were added to WO_3 were shown in **Figures 3** and **4**, respectively. In **Figure 3**, the peak intensity of WO_3, which is a characteristic of crystallization, rises with increasing calcination temperatures. This means that the crystallinity is enhanced at higher calcination temperature. By comparing the data we obtained with those of JCPDS as reference data, we concluded that the experimental data were agreed with an orthorhombic structure, which is one of the possible structures of WO_3 [13]. In **Figure 4**, new peaks started to appear at characteristic 2θ values as metal catalysts and metal oxides were added.
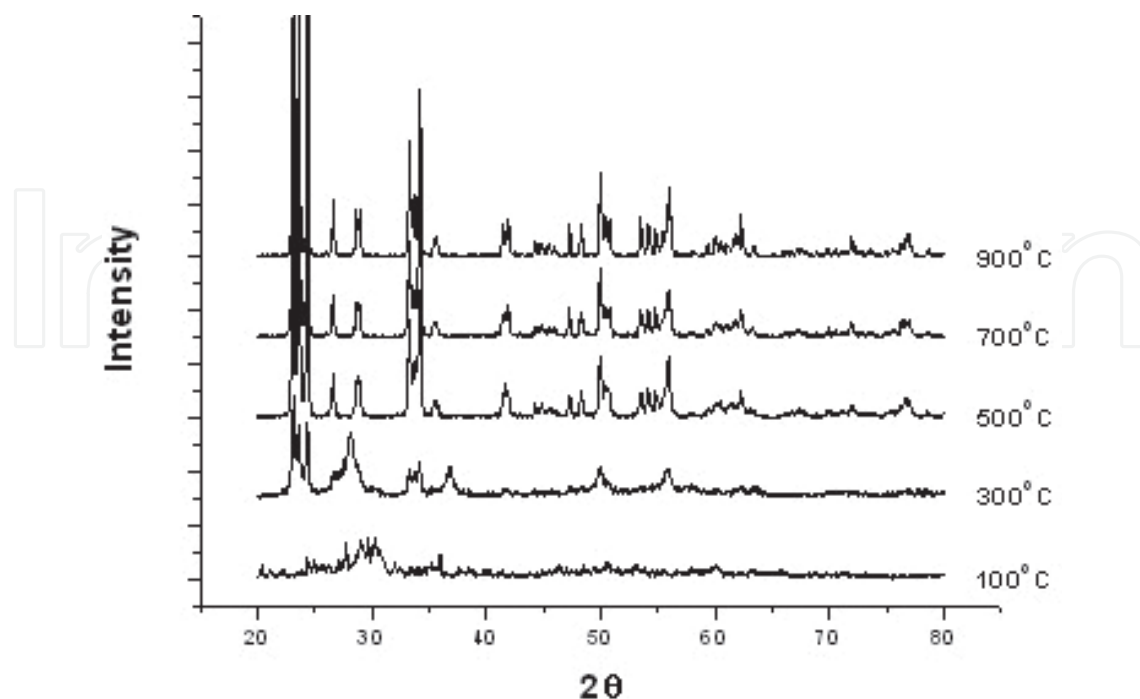

Figure 3. X-ray diffraction patterns of WO_3 powder with temperature.
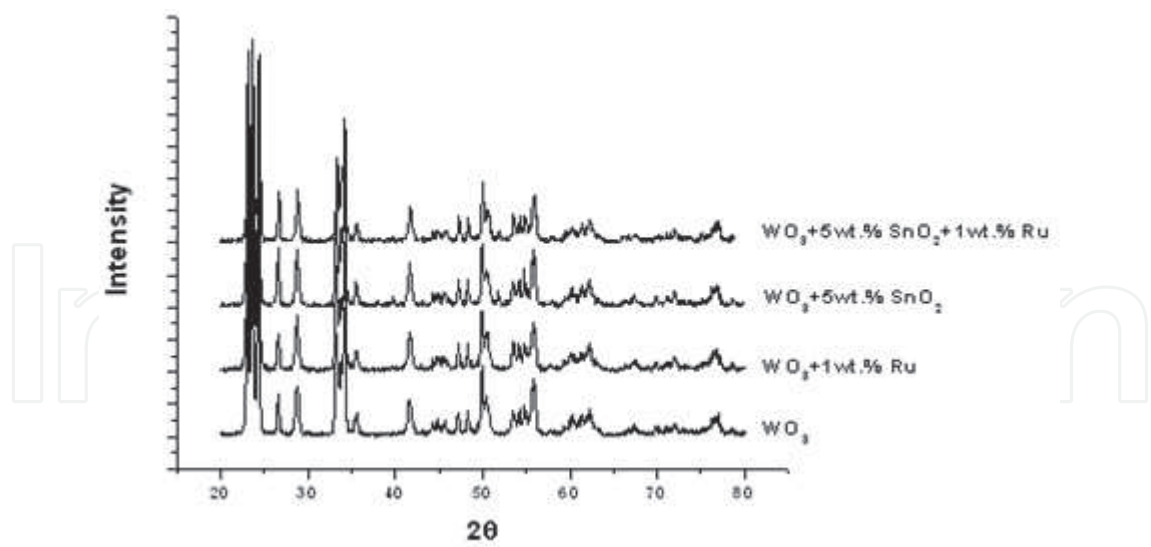
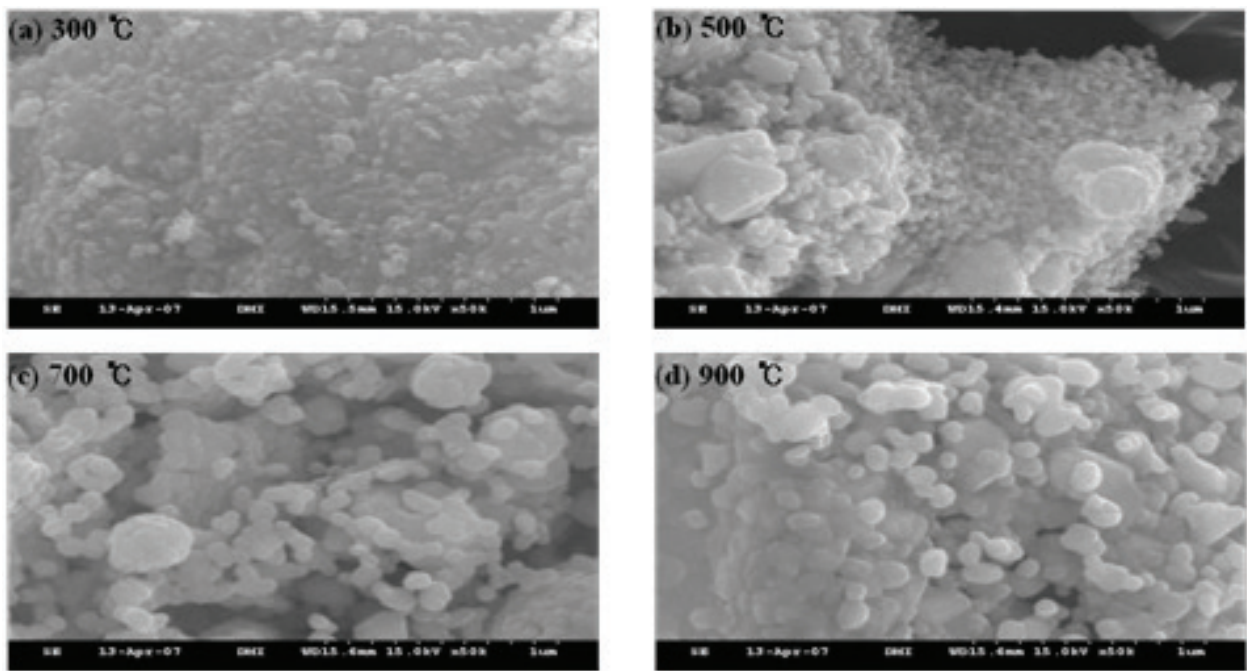**Figure 4.** X-ray diffraction patterns of the various sensor materials based on catalyst/SnO$_2$/WO$_3$.

Figure 5. SEM image of WO3 powders calcined for 2 h at (a) 300°C, (b) 500°C, (c) 700°C and (d) 900°C.

Figure 5 exhibits SEM images of the WO$_3$ thick film at various calcination temperatures. These SEM images show that the particle size of the WO$_3$ thick film increases with rising calcination temperatures.

Figure 6 represents SEM images and EDS results of each sensing material composed of WO$_3$ containing metal oxides and metal catalysts. **Figure 6a** shows SEM photos and EDS results for sensor material of WO$_3$ only. **Figure 6(b), (c)**, and **(d)** shows SEM photos and EDS data for sensor materials of 5 wt% SnO$_2$/WO$_3$, 1 wt% Ru/WO$_3$, and 1 wt% Ru/5 wt% SnO$_2$/WO$_3$, respectively. The SEM photos obviously show the surface morphology of each

sensor material. The EDS data indicate the appearance of new peaks of the component in each sensor material.

3.1.2. The H_2S gas sensor

A sensing material for gas detection was fabricated with various mixing ratios of the main material SnO_2, metal oxide and catalyst. The techniques of SEM, EDS, XRD and BET were employed to analyze surface morphology, component, the degree of crystallinity, phase and surface area of each fabricated sensing material. **Figure 7** shows the XRD patterns of the SnO_2 synthesized by sol-gel method and SnO_2 mixed with catalyst and metal oxide.

By a comparison of the data of SnO_2 we obtained in this experiment with those in JCPDS, we presume the structure to be rutile form which is shown in **Figure 7**. As for the sample of SnO_2 mixed with 10 wt% WO_3, a new peak was appeared around 2θ. Referring to the data in JCPDS, the data of WO_3 tell us that the structure is orthorhombic among the three possible structures. Based on the interpretation of peaks of SnO_2, we can say that there was no specific phase change. Any new 2θ value was not also observed in the diffraction pattern for the sample of SnO_2 mixed with 10 wt% WO_3/1 wt% Ru. This implies that 1 wt% of Ru was not sufficient to produce a crystalline peak of Ru.

Table 1 shows the measured results of specific surface areas of SnO_2 in which pure SnO_2 was mixed with 10 wt% WO_3 and various metal catalysts. Compared to pure SnO_2, SnO_2 with added 10 wt% WO_3 and various metal catalysts showed larger BET surface areas, pore diameters and pore volumes. This means that SnO_2 added with WO_3 and metal catalyst hindered the particle growth, which results in increasing the specific surface area.

In particular, the SnO_2 powder (in which 10 wt% WO_3 was mixed with 1 wt% Ru) showed the highest BET specific surface area, pore diameter and total pore volume. The sensor fabricated with this material showed good functional properties, including response, reaction, recovery and selectivity.

SEM photos and EDS data for SnO_2 powder added with WO_3 and various metals were shown in **Figure 8**. In SEM photos, the surface morphology of each sensing material could be observed, and the peak of the component element for each sensing material was verified by the EDS data.

3.1.3. The toluene gas sensor

This study produced sensor material for gas detection by varying the mixing ratios of SnO_2 powder as main material, ZnO, transition metal catalyst and carbon black. The crystal property of each produced sensor material was analyzed by using XRD measurements. **Figure 9** shows each XRD pattern of various sensor materials such as SnO_2 synthesized by the precipitation method, SnO_2/ZnO which is SnO_2 with 20 wt.% ZnO, SnO_2/ZnO/Cu which is SnO_2/ZnO added of 1 wt.% Cu and SnO_2/ZnO/Cu/carbon black which is SnO_2/ZnO/Cu added of 5 wt.% carbon black. When the experimental data were compared to various values of SnO_2 and ZnO in JCPDS, it was confirmed that the peaks were characteristic of the crystal structure held by SnO_2 and ZnO. Meanwhile, it was not possible to confirm the peak of Cu and carbon black. The XRD
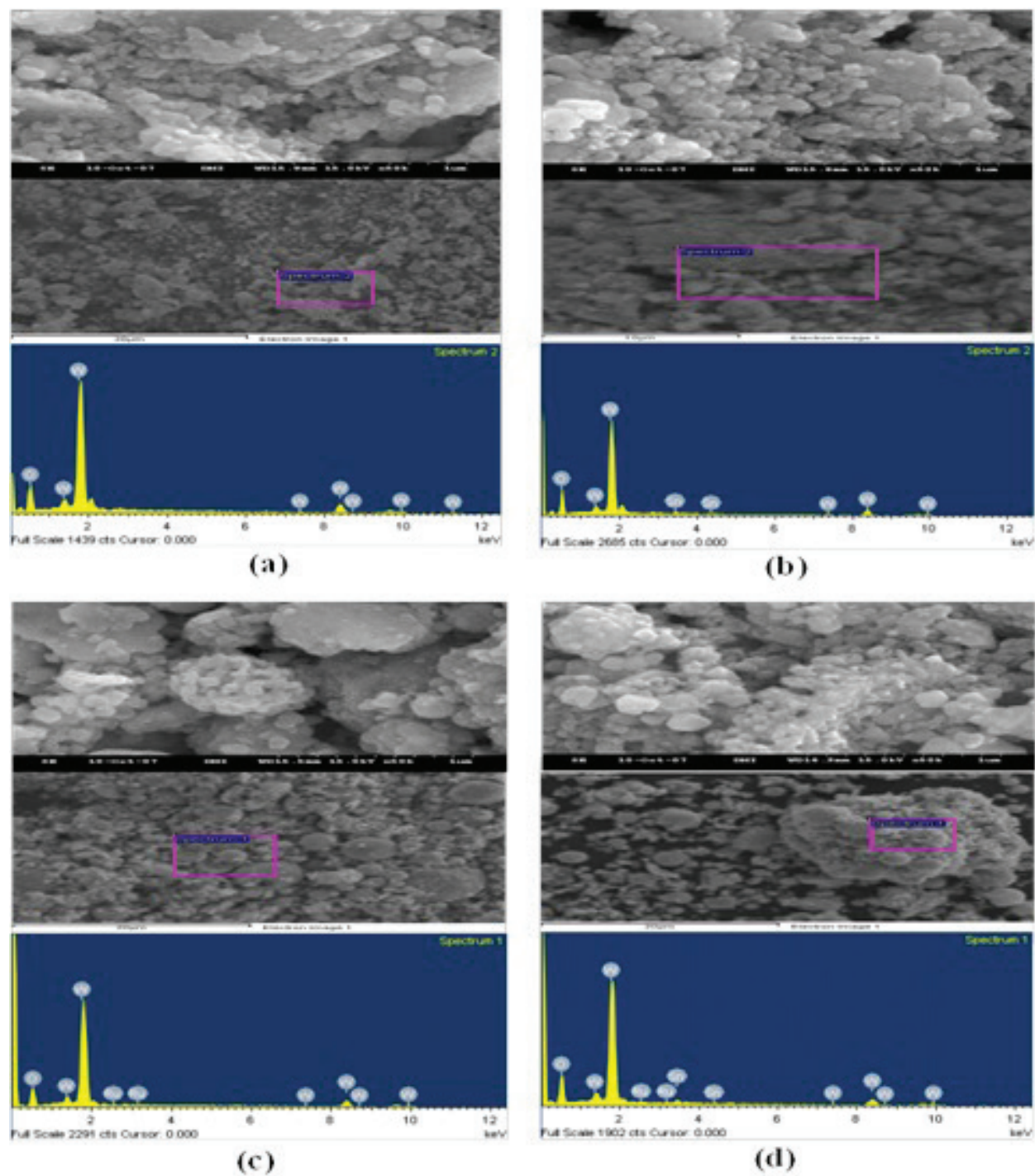
Figure 6. SEM images and EDS results of sensing materials. Upper: SEM (×50 K), middle: SEM (5 K) and lower: EDS (×5 K).

peak for Cu was not available because only small amount of Cu at 1 wt.% was added. The XRD peak for carbon black was not available because carbon black is a weak crystalline material.

Figure 10 shows SEM images taken at 100,000 magnification showing ratios of SnO_2, $SnO_2/20\%ZnO$, $SnO_2/20\%ZnO/1\%Cu$ and $SnO_2/20\%ZnO/1\%Cu/5\%$ carbon black, respectively.
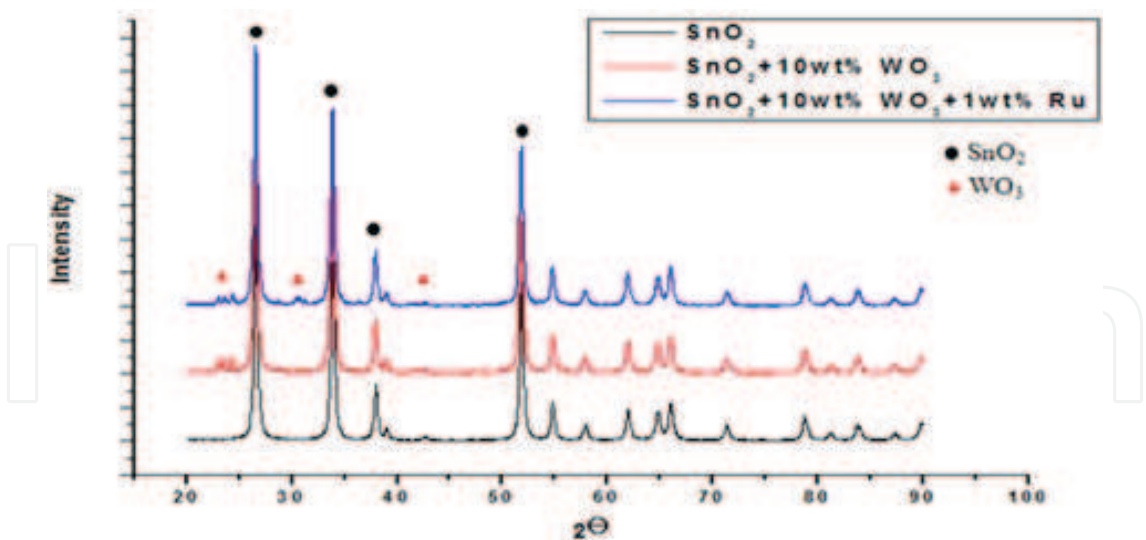
Figure 7. XRD patterns of catalyst/WO_3/SnO_2 powder.

Samples	BET surface area (m²/g)	Pore diameter (nm)	Total pore volume (cm³/g)
SnO_2	7.16	12.3	0.1218
1 wt% Ru-10 wt% WO_3/SnO_2	13.06	31.6	0.1398
1 wt% Pd-10 wt% WO_3/SnO_2	10.73	3.795	0.09435
1 wt% Au-10 wt% WO_3/SnO_2	10.64	21.01	0.09975
1 wt% In-10 wt% WO_3/SnO_2	11.53	26.92	0.1202
1 wt% Ag-10 wt% WO_3/SnO_2	11.39	22.34	0.09927

Table 1. Surface area (m²/g), pore diameter (nm), pore volume (cm³/g) of catalysts/WO_3/SnO_2.
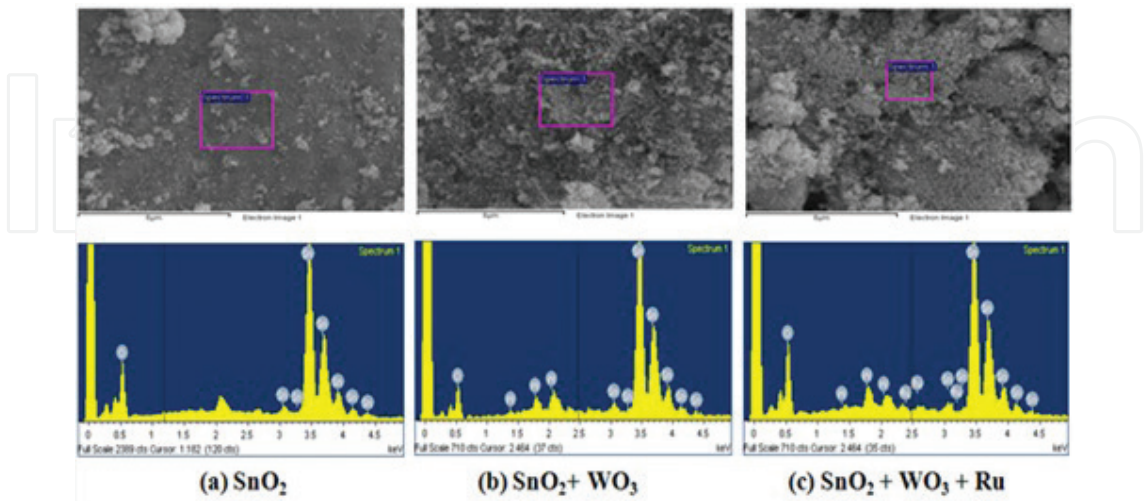
Figure 8. SEM images and EDS results of gas-sensing materials. (a) SnO_2, (b) 10 wt% WO_3/SnO_2 and (c) 1 wt% Ru/10 wt% WO_3/SnO_2.
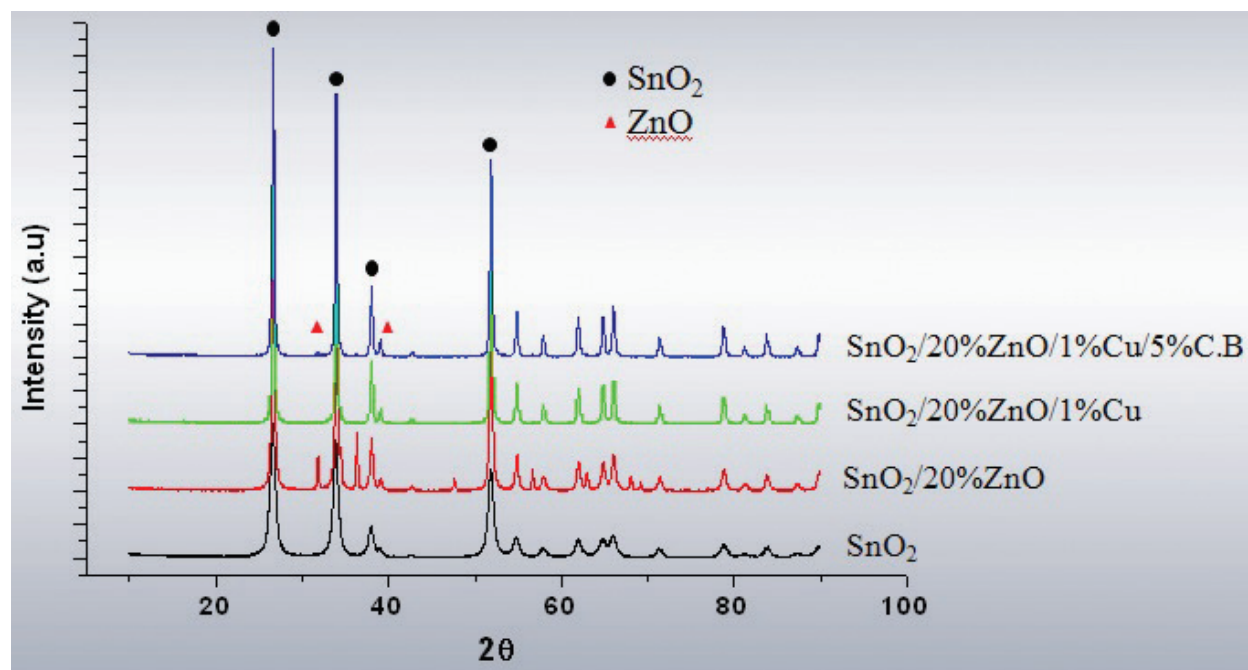
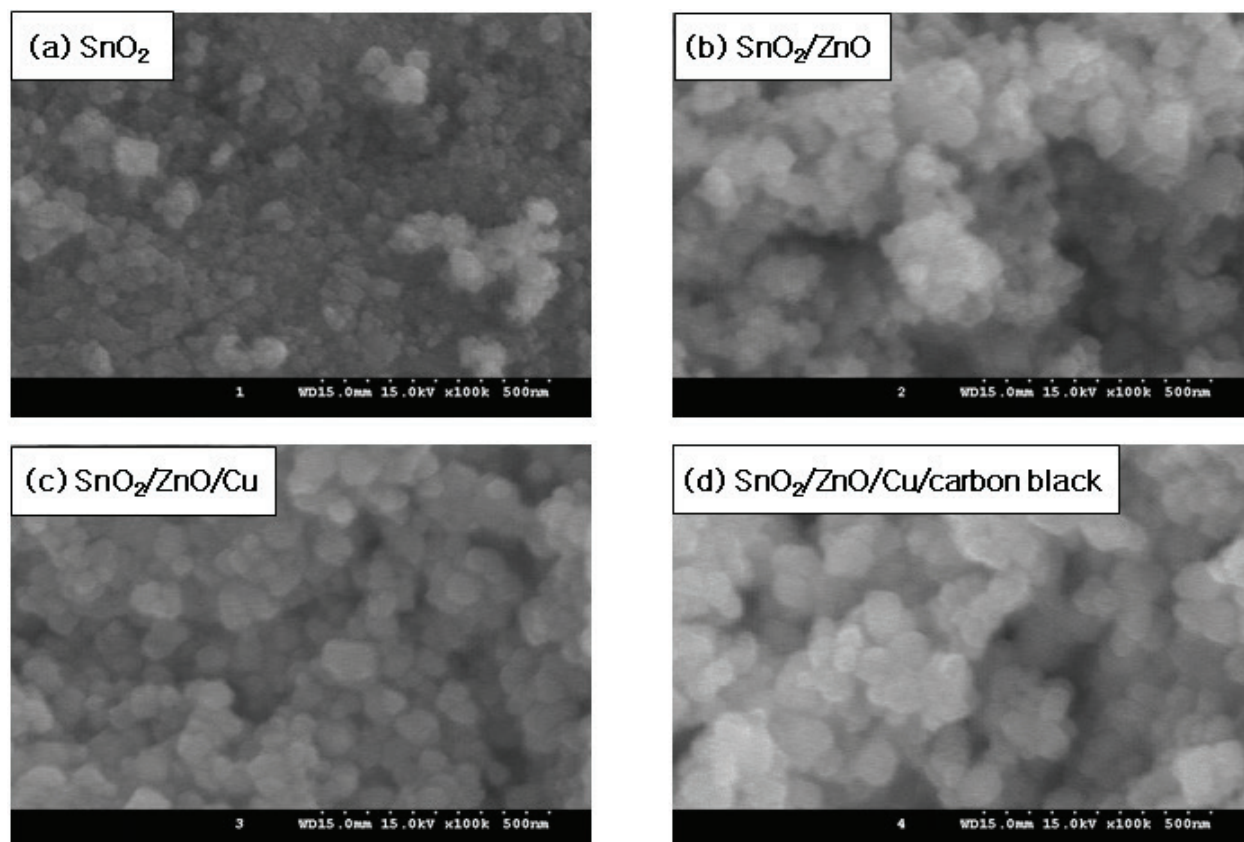**Figure 9.** XRD patterns of the various sensor materials.

Figure 10. SEM images of the various sensor materials.

From these SEM images, it could be seen that the sensor material made of $SnO_2/20\%ZnO/1\%Cu/5\%$ carbon black had uniform particle sizes and crystallinities compared to other sensor materials.

Figure 11 shows the SEM images and EDS measurements for each sensor material composed of SnO_2, $SnO_2/20\%ZnO$, $SnO_2/20\%ZnO/1\%Cu$ and $SnO_2/20\%ZnO/1\%Cu/5\%$ carbon black, respectively. It was possible to observe the surface state of each sensor material through studying the SEM images shown in **Figure 11**. It was also possible to confirm the peaks of component elements existing in each sensor material from the EDS results. The existence of Sn and O was confirmed in **Figure 11(a)**; the existence of Sn, O and Zn was confirmed in **Figure 11(b)**; the existence of Sn, O, Zn and Cu was confirmed in **Figure 11(c)** and the existence of Sn, O, Zn, Cu and C was confirmed in **Figure 11(d)**.

3.2. Response characteristics to acetaldehyde gas

Figure 12 shows the sensing characteristics of WO_3 thick film sensor to acetaldehyde (100 ppm) at the various operating and calcination temperatures. In particular, WO_3 calcined at 500°C is shown to give the best sensitivity at 350°C. The sensing characteristics of the sensor after addition of SnO_2 and metal catalyst to acetaldehyde gas (100 ppm) at various operating temperatures were shown in **Figure 13**. While the highest sensitivity was reached at 350°C in the case of WO_3 alone, this sensitivity peak occurred at 300°C in the presence of additional constituents, that is, SnO_2 and Ru. This can be understood as follows: at a given temperature, the activation energy changes greatly depending on the amount of SnO_2 and the kind of metal catalyst added. Because the sensitivity of a sensor degrades with the temperature higher than 300°C, the experiments were carried out at a fixed operation temperature of 300°C.

Metal catalysts were added to the sensor material in order to improve the sensitivity and selectivity of the gas sensor to acetaldehyde gas. Mixing a metal catalyst with a metal oxide
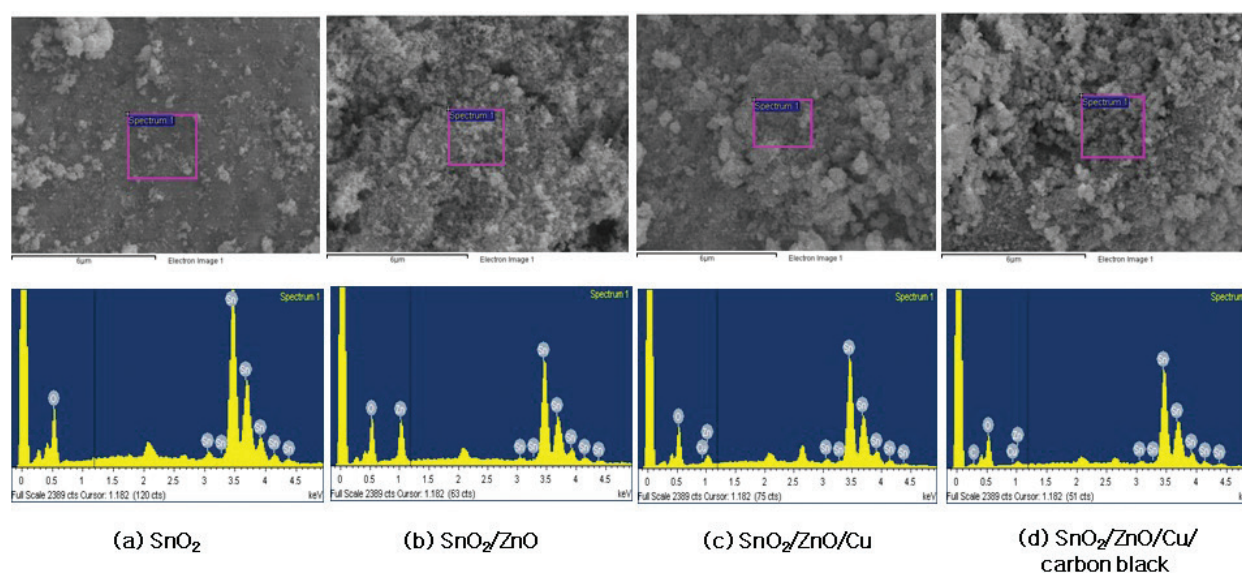

(a) SnO_2 (b) SnO_2/ZnO (c) $SnO_2/ZnO/Cu$ (d) $SnO_2/ZnO/Cu/$ carbon black

Figure 11. SEM images and EDS results of the various sensor materials.

induces an increase in the adsorption species caused by the activation of electrons. This affects the adsorption-desorption process, which results in an enhancement of electrical conductivity. To improve the effect of this catalytic reaction, the contacting area of metal catalysts with the sensor needs to be increased. Such a move has been found to greatly affect sensitivity, selectivity and operational temperature in terms of sensing the amount of gas [14].

Figure 14 depicts the sensing characteristics of sensor materials to acetaldehyde gas with various metal catalysts. The metal catalysts were added to 5 wt% SnO_2/WO_3, which was used as main sensor material. As shown in **Figure 14**, the sensor material containing 1 wt% of Ru gives better sensitivity than those of other catalysts. This explains that 5 wt% SnO_2/WO_3 with a metal catalyst of 1 wt% Ru shows better selectivity in oxidizing acetaldehyde gas
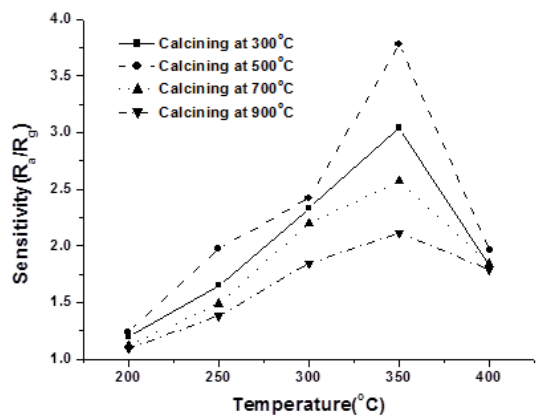

Figure 12. The sensitivity of WO_3 thick films with various calcination temperatures for acetaldehyde gas (100 ppm) with different operating temperatures.
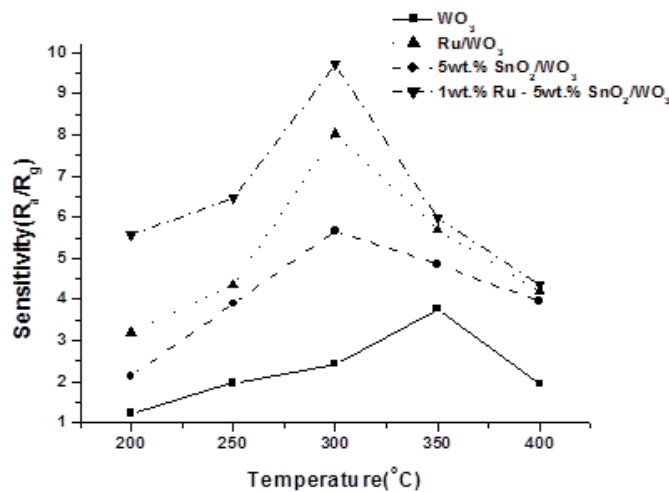

Figure 13. The sensitivity of the gas sensor for acetaldehyde gas (100 ppm) at various temperatures.

than any other sensing materials. The reason we used 1 wt% concentration is that it gave the best sensitivity, that is, in the range of 0–1 wt%, the sensitivity increases with elevated Ru concentrations. On the other hand, if the concentration exceeds 1 wt%, there is a decrease in sensitivity. In this case, the Ru particles were not able to spread homogenously on the surface of the thick film due to the coagulation.

Figure 15 shows the results of the selectivity study of the sensing materials giving with the best selectivities toward acetaldehyde gas compared to various other volatile organic compounds. The sensitivity measurement of 1 wt% Ru/5 wt% SnO_2/WO_3 gas sensor which showed the best sensitivity to acetaldehyde gas was performed within a concentration range of 100 ppm. The result showed that the sensitivity to acetaldehyde gas was much higher than other gases. It means that the sensing material of 1 wt% Ru/5 wt% SnO_2/WO_3 works better for acetaldehyde gas in decomposing and activating reaction than for other VOC gases.

3.3. Sensing characteristics to H_2S gas

The sensing response of WO_3/SnO_2 was investigated for different type of sensor materials where the amounts of metal catalyst added were varied. The kinds of catalyst were selected to give a good response and selectivity to H_2S gas. In general, metal catalyst mixed with metal oxide helps to transfer electrons smoothly and increases the number of absorbed species in the absorption process, which lead to the change of electric conductivity on the sensor material. It has also been known that increasing the contact area affects the catalyst to enhance the response, selectivity and operating temperature of the sensor [15].

Figure 16 shows the response of hydrogen sulfide across different metal catalysts. Various metal catalysts were added to the basic sensor material composed of 10 wt% WO_3/SnO_2. As shown in **Figure 16**, the sensor material with added 1 wt% Ru compared to other metal catalysts, and the operating temperature was 200°C, which represented a reduction of 50°C. This meant that 1 wt% Ru/10 wt% WO_3/SnO_2 sensor material oxidized hydrogen sulfide better than other sensor materials and also showed better selectivity.
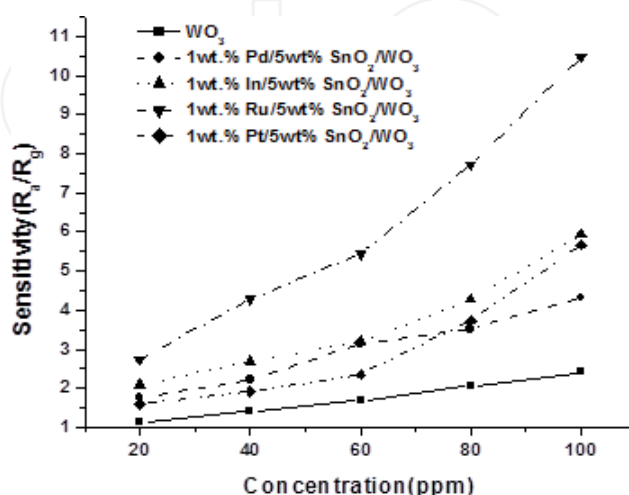

Figure 14. Sensitivity of catalyst/5 wt% SnO_2/WO_3 to various concentration of acetaldehyde gas at 300°C.
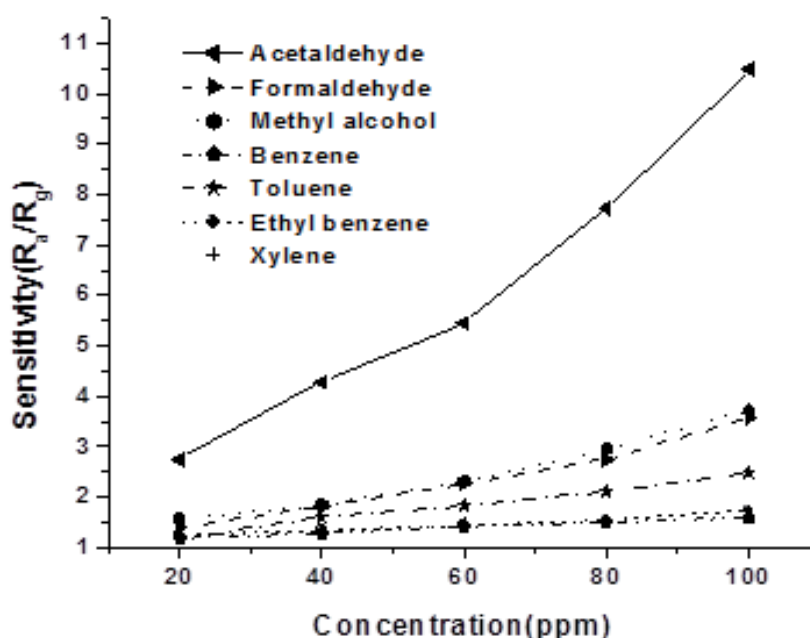
Figure 15. The sensitivity of 1 wt% Ru/5 wt% SnO$_2$/WO$_3$ to various gases (100 ppm) at 300°C.

Figure 17 shows the sensing response of H$_2$S gas for the samples of various amount of metal catalysts added to find the optimal condition. For the main sample of 10 wt% WO$_3$/SnO$_2$, the sensing response was examined by varying the amount of Ru catalyst added in the range of 0.5–5.0 wt%, and it was found to be the best for the case of 1 wt% Ru addition. When the quantity of catalyst was below 1 wt%, it is not sufficient to activate the reaction. While the quantity of catalyst was above 1 wt%, the Ru particles aggregated itself and changed the characteristics of sensor material which did not further improve responses.

Figure 18 shows the response comparing the changes in different concentration levels of 100 ppm of hydrogen sulfide at 200°C when SnO$_2$ was mixed with 10 wt% WO$_3$ + 1% Ru. Finally, the sensor material of 1 wt% Ru/10 wt% WO$_3$/SnO$_2$ showed the best response characteristics.

Figure 19 presents the selectivity results of various gases based on the sensor material showing the best sensitivity for H$_2$S gas. The sensor prepared with the material of 1 wt% Ru/10 wt% WO$_3$/SnO$_2$ showed the best sensitivity and was tested its sensitivities to various gases at an operating temperature of 200°C and the concentration range of 20–100 ppm. As a result, the sensor showed better response to H$_2$S gas than to other gases. Therefore, it is known that 1 wt% Ru/10 wt% WO$_3$/SnO$_2$ adsorbs H$_2$S gas well and enhances the catalytic reaction to improve the selectivity.

3.4. Response characteristics to toluene gas

Carbon black is a material made by covalent bonding of carbon. It is known that carbon black has good electric conductivity and good thermal conductivity. There is existing literature
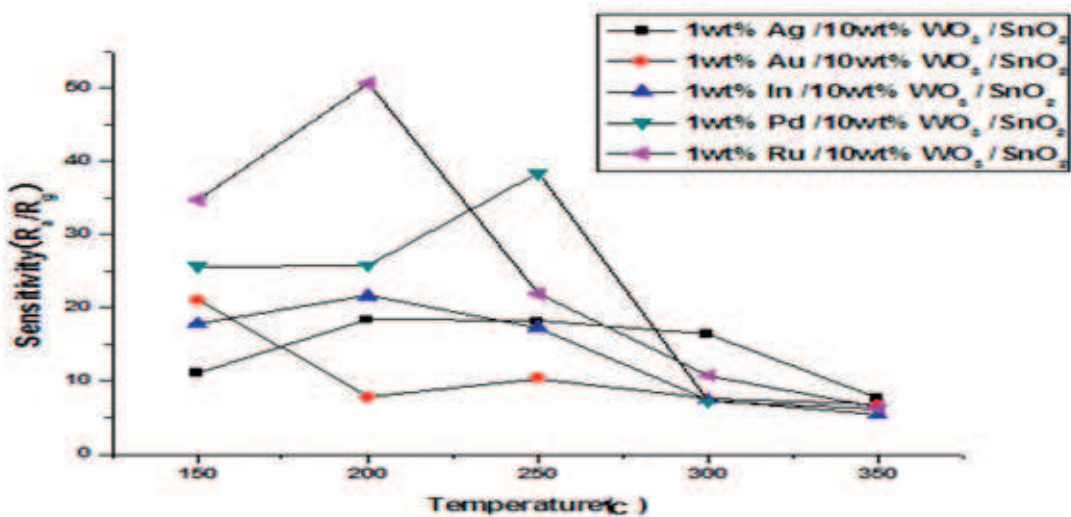
Figure 16. Response with catalysts/10 wt% WO_3/SnO_2 to the hydrogen sulfide gas (100 ppm) at different operating temperatures.
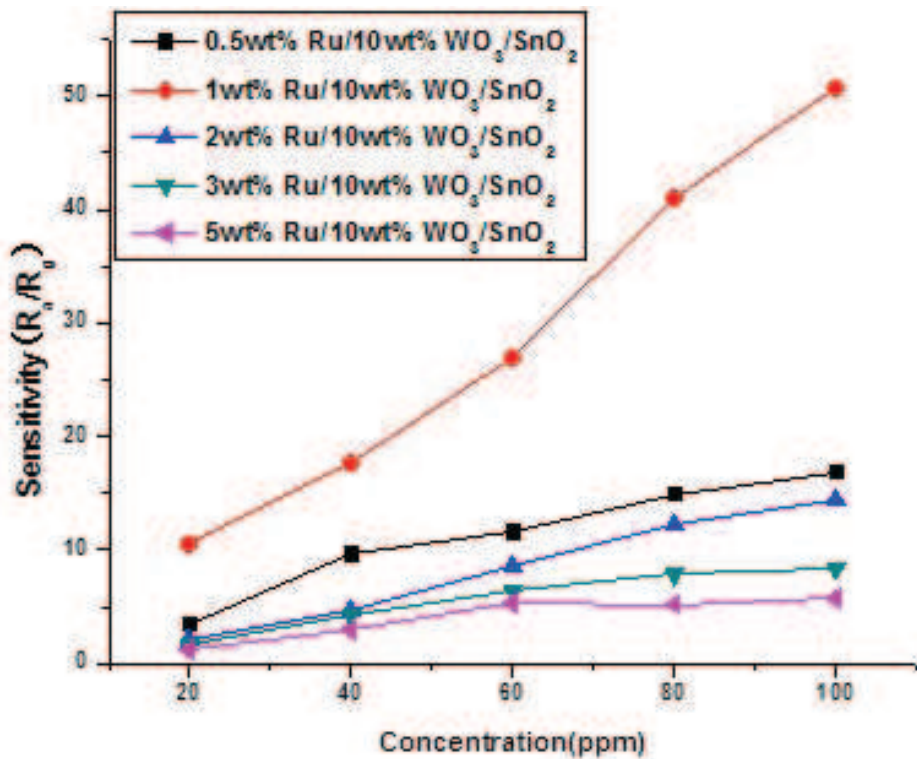

Figure 17. Sensitivity with the catalyst/WO_3/SnO_2 to the various concentrations of hydrogen sulfide gas at 200°C.

study that reported the addition of carbon black on sensor material to decrease sensor operation temperature [16–18]. In this study, carbon black is added to sensor material to decrease operation temperature and increase the sensitivity of the sensor. **Figure 20** is the sensitivity on 100 ppm toluene gas depends on carbon black added quantity. As seen in the figure, the
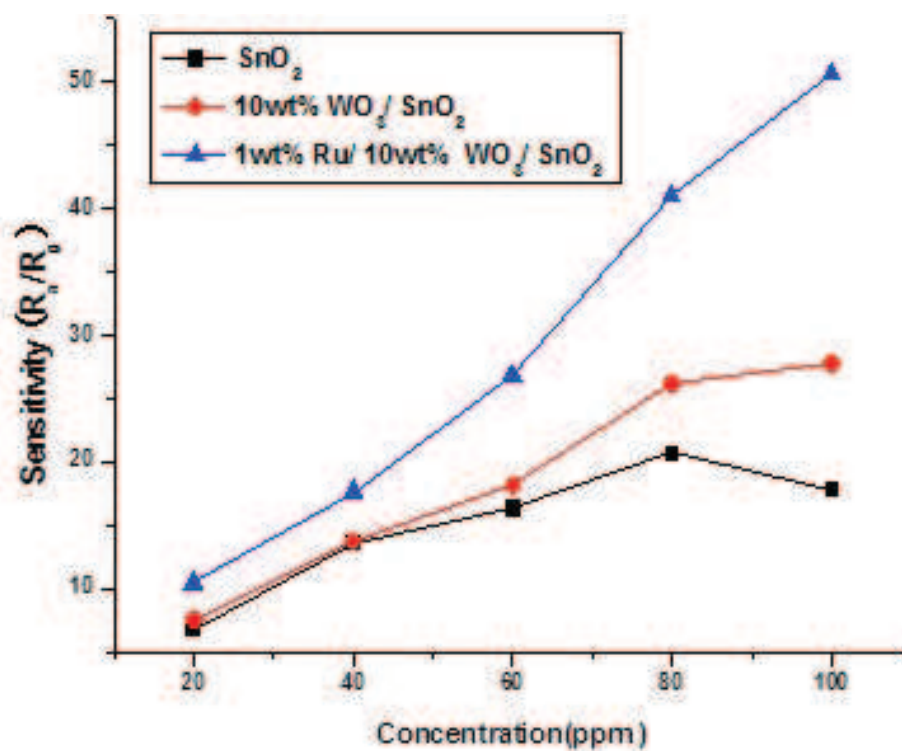
Figure 18. The sensitivity of 1 wt% Ru/10 wt% WO$_3$/SnO$_2$ from 20 ppm to 100 ppm of hydrogen sulfide gas at 200°C.
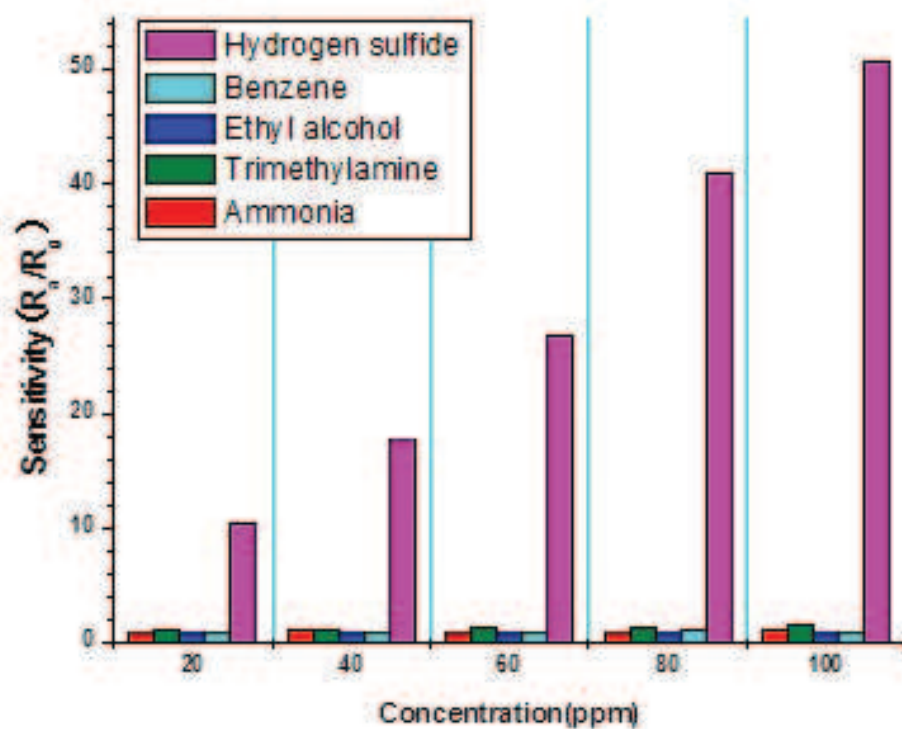

Figure 19. Sensitivity of 1 wt% Ru/10 wt% WO$_3$/SnO$_2$ to the various concentrations of various gases at 200°C.
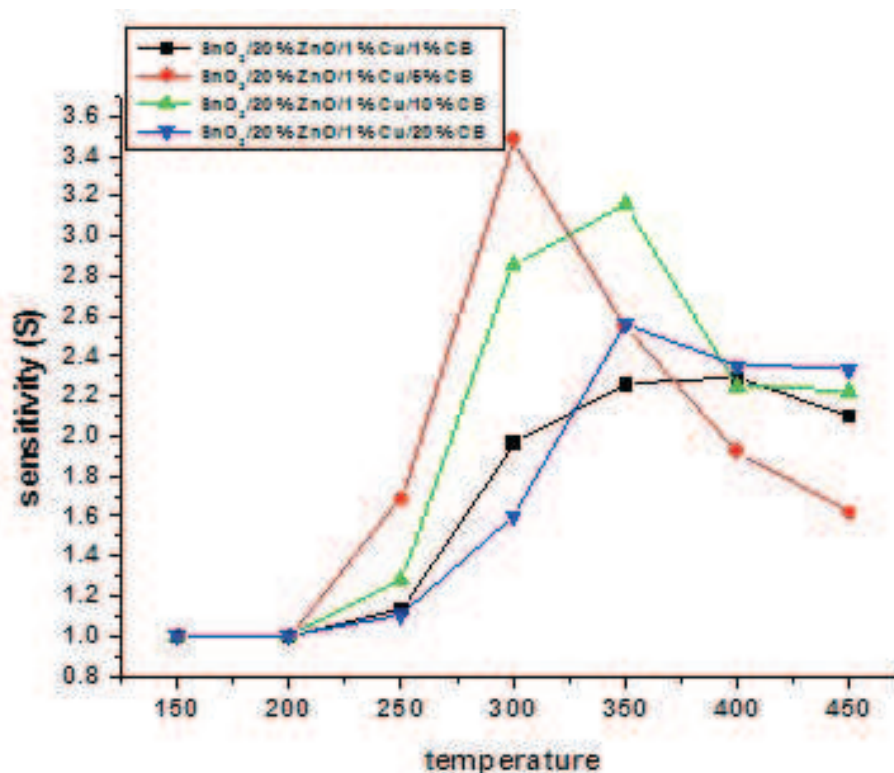
Figure 20. Sensitivity of sensors with various contents of carbon black to the toluene gas (100 ppm) at various temperatures.

sensitivity of sensor fabricated with material added of 5 wt.% carbon black of SnO_2 has better sensitivity and 50°C lower operation temperature compared to sensors fabricated with material added of different wt% of carbon black. The reason is believed that the sensor sensitivity and operation temperature decreased by the increase in heat dispersion in sensor material when carbon black was added.

Figure 21 is the sensitivity measurement on 100 ppm toluene gas using a sensor fabricated with different components such as SnO_2, $SnO_2/20\%ZnO$, $SnO_2/20\%ZnO/1\%Cu$ and $SnO_2/20\%ZnO/1\%Cu/5\%$carbon black. As seen in the figure, the sensor fabricated with $SnO_2/20\%ZnO/1\%Cu/5\%$carbon black has better sensitivity and lower operation temperature compared to sensors produced with other three materials.

Figure 22 is the sensitivity measurement on 1–20 ppm low concentration toluene gas using a sensor made of $SnO_2/20\%ZnO/1\%Cu/5\%$carbon black, which showed the best sensitivity in this study. This sensor showed a linear increase in sensitivity at a concentration of 20 ppm or less in general.

Figure 23 is the selectivity on various volatile gases of the sensor fabricated with $SnO_2/20\%ZnO/1\%Cu/5\%$carbon black, which showed the best sensitivity on toluene gas in this study. Sensitivity was measured on various gases at 300°C operation temperature and 10–100 ppm concentration range. The result suggested that the sensor had the best sensitivity on toluene gas compared to the sensitivity to other gases. There was some interference effect
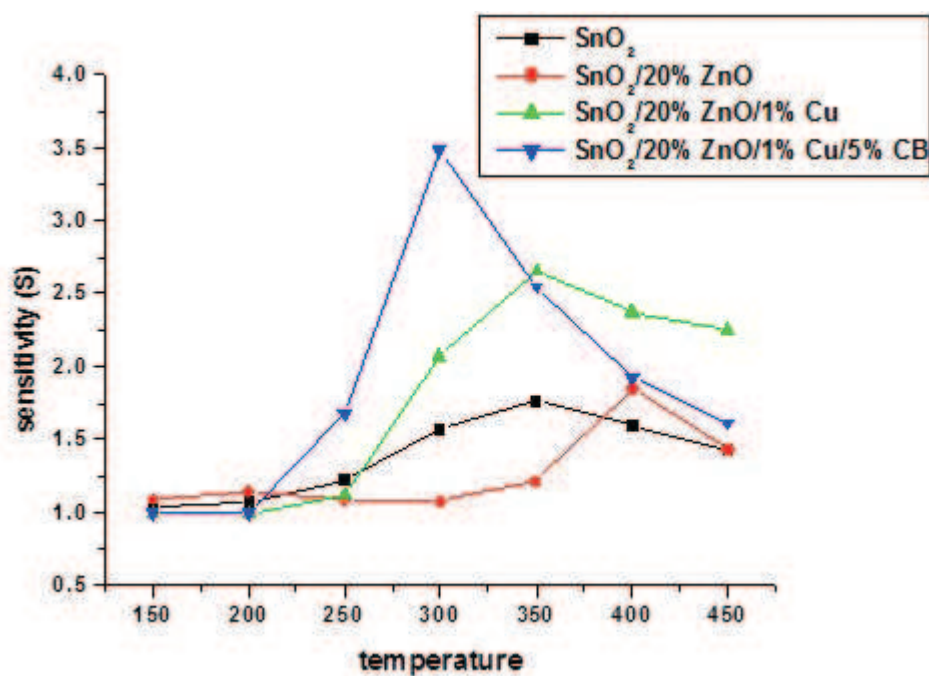
Figure 21. Sensitivity of the SnO$_2$/20%ZnO/1%Cu/5% carbon black sensor for toluene gas (100 ppm) to the various temperatures.
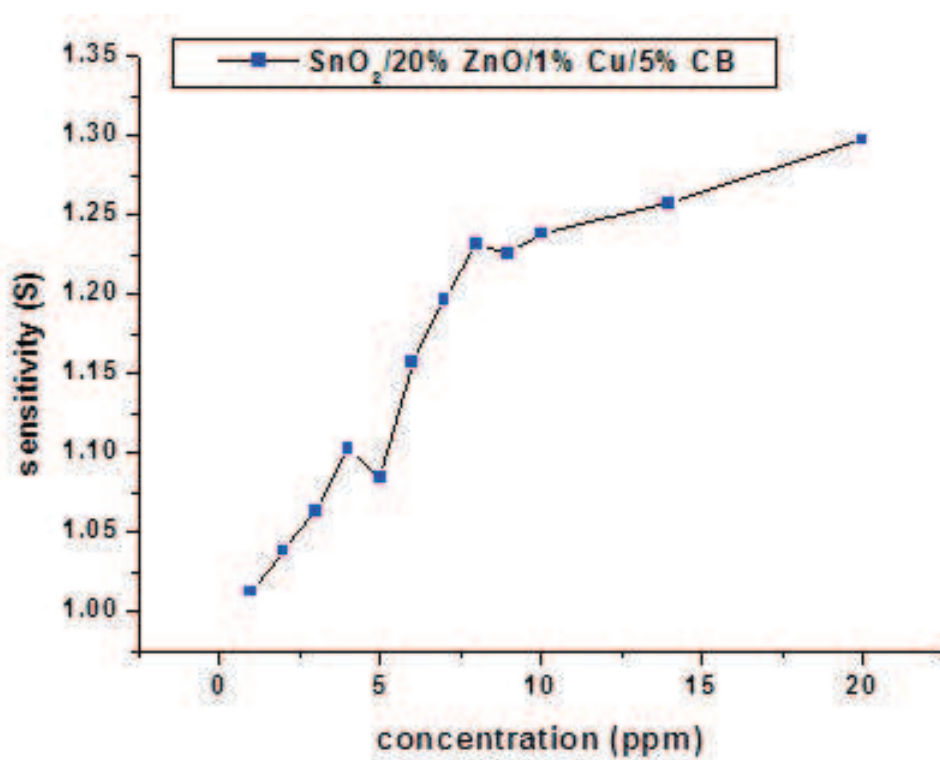

Figure 22. Sensitivity of SnO$_2$/20%ZnO/1%Cu/5%carbon black sensor from 1 to 20 ppm of toluene gas at 300°C.
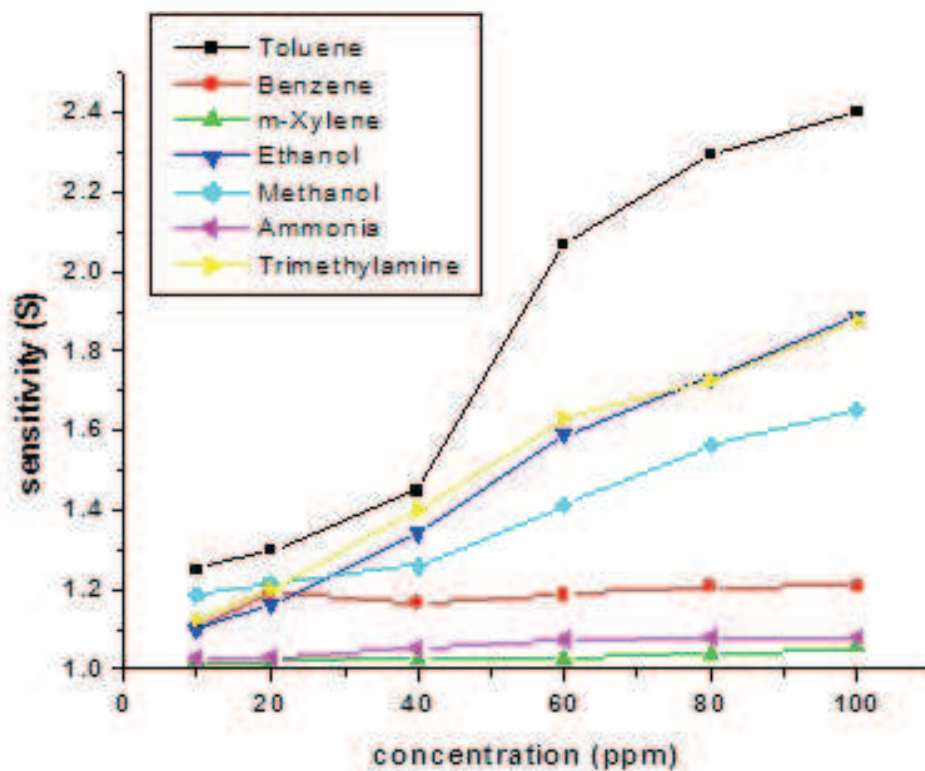
Figure 23. Sensitivity of SnO_2/20%ZnO/1%Cu/5%carbon black to the various gases at 300°C.

from ethanol and trimethylamine gas; however, interference effect from other volatile gases was not so significant. A sensor fabricated with SnO_2/20%ZnO/1%Cu/5%carbon black has better selectivity on toluene gas, because it decomposes more toluene gas and activates more reaction compared to other volatile gas.

4. Conclusion

Semiconductor metal oxide gas sensors can be used for diverse applications, ranging from equipment to monitor environmental and occupational safety to facilitating quality assurance through novel measurement. The nature of the gas-sensitive material and the concentration of the target gas (usually a few ppb–ppm) will determine the measuring range and limitations of the device.

In this study, the metal oxide gas sensor was fabricated with SnO_2 and WO_3 as the basic substances added to the metal oxide (SnO_2, WO_3, and ZnO) and various metal catalysts to detect the toxic gas. By changing the added amount and types of metal oxide and catalysts, this study investigated the sensitivity, operating temperature and recovery properties for the toxic gas.

(1) The sensing characteristics of the fabricated gas sensors added with catalysts and metal oxides to SnO_2 tend to rely on the operating temperature, calcination temperature and the kind and composition of the catalyst and metal oxide.

(2) The optimal conditions for the fabrication of the sensor material for detecting acetaldehyde gas were known to be 300°C as an operation temperature, 500°C as a calcination temperature, 20 μm as a film thickness and ethylene glycol as a binder. The best sensitivity, selectivity and response-recovery characteristics were achieved when 1 wt% Ru/5 wt% SnO_2 was added to the WO_3 sensing material.

(3) The sensing characteristics of hydrogen sulfide gas sensor made by adding catalyst and metal oxide to SnO_2 tend to rely on the operating temperature, calcination temperature and kind and composition of catalyst and metal oxide. The ideal condition for the sensor material to detect H_2S gas is temperatures of 200°C for operation and 600°C for calcination, and the sample of SnO_2 added with 10 wt% WO_3 and 1 wt% Ru.

(4) The optimum conditions for the toluene gas detection sensor are an operating temperature of 300°C with added metal catalyst Cu and carbon black. The best sensitivity and highest selectivity were achieved with 20% ZnO, 1% Cu and 5% carbon black, in terms of wt% to SnO_2 added to SnO_2 by impregnation.

Acknowledgements

Author details

Chang-Seop Lee* and Yong Jae Kim

*Address all correspondence to: surfkm@kmu.ac.kr

Department of Chemistry, Keimyung University, Daegu, South Korea

References

[1] Wark K, Warner CF. Air Pollution: Its Origin and Control. New York: Haper Collins; 1981

[2] Noordally E, Richmond JR, Tahir SF. Destruction of volatile organic compounds by catalytic oxidation. Catalysis Today. 1993;**17**(1–2):359–366

[3] Hodgson AT, Faulkner D, Sullivan DP, DiBartolomeo DL, Russell ML, Fisk WJ. Effect of outside air ventilation rate on volatile organic compound concentrations in a call center. Atmospheric Environment. 2003;**37**(39–40):5517–5527

[4] Min BK, Choi SD. Development of methane gas sensor by various powder preparation methods. Journal of the Korean Ceramic Society. 1999;**5**(2):125–130

[5] Lim CB, Oh SJ. Microstructure evolution and gas sensitivities of Pd-doped SnO_2-based sensor prepared by three different catalyst-addition processes. Sensors and Actuators B: Chemical. 1996;**30**(3):223–231

[6] Yoo DJ, Tamaki J, Miura N, Yamazoe N, Park SJ. Effect of film thickness on gas sensing behavior of thin-film-type gas sensor. Korean Journal of Materials Research. 1996;**6**(7):716–722

[7] Acosta DR, Zironi EP, Montoya E, Estrada W. About the structural, optical and electrical properties of SnO_2 films produced by spray pyrolysis from solutions with low and high contents of fluorine. Thin Solid Films. 1996;**288**(1–2):1–7

[8] Serrini P, Briois V, Horrillo MC, Travers A, Manes L. Chemical composition and crystalline structure of SnO_2 thin films used as gas sensors. Thin solid Films. 1997;**304**(1–2):113–122

[9] Qi Q, Zhang T, Liu L, Zheng X. Improved NH_3, C_2H_5OH, and CH_3COCH_3 sensing properties of SnO_2 nanofibers by adding block copolymer P123. Sensors and Actuators B. 2009;**141**(1):174–178

[10] Zeng Y, Zhang T, Wang L, Kang M, Fan H, Wang R, He Y. Enhanced toluene sensing characteristics of TiO_2-doped flowerlike ZnO nanostructures. Sensors and Actuators B. 2009;**140**(1):73–78

[11] Song X, Zhang D, Fan M. A novel toluene sensor based on ZnO–SnO_2 nanofiber web. Applied Surface Science. 2009;**255**(16):7343–7347

[12] Kawahara A, Katsuki H, Egashira M. Fabrication of semiconductor oxide thick films by slide-off transfer printing and their NO_2-sensing properties. Sensors and Actuators B. 1998;49(3):273–278

[13] Khadayate RS, Sali JV, Patil PP. Acetone vapor sensing properties of screen printed WO_3 thick films. Talanta. 2007;**72**(3):1077–1081

[14] Xu C, Kurokawa J, Miura N, Yamazoe N. Stabilization of SnO_2 ultrafine particles by additives. Journal of Materials Science. 1992;**27**(4):963–971

[15] Dean JA. Lange's Handbook of Chemistry. 12th ed. New York: McGraw Hill; 1979. pp. 10–54

[16] Yamazoe N, Kurokawa Y, Seiyama T. Effects of additives on semiconductor gas sensors. Sensors and Actuators. 1983;**4**:283–289

[17] Yamazoe N. New approaches for improving semiconductor gas sensors. Sensors and Actuators B: Chemical. 1991;**5**(1–4):7–19

[18] Yamazoe N, Miura N. Some basic aspects of semiconductor gas sensors. Chemical Sensor Technology. 1992;**4**:19–42